2178 *Chem. Mater.* **2010,** *22,* 2178–2180
DOI:10.1021/cm100139d

CHEMISTRY OF MATERIALS
Communication

Ammonia-Treated Ordered Mesoporous Carbons as Catalytic Materials for Oxygen Reduction Reaction

Xiqing Wang,[†,‡] Je Seung Lee,[†,‡] Qing Zhu,[†,‡] Jun Liu,[§] Yong Wang,[§] and Sheng Dai*[,†]

[†]*Chemical Sciences Division, Oak Ridge National Laboratory, Oak Ridge, Tennessee 37831-6201, and* [§]*Pacific Northwest National Laboratory, Richland, Washington 99352.* [‡]*These authors contributed equally to this work*

Received January 16, 2010
Revised Manuscript Received March 6, 2010

Polymer electrolyte membrane fuel cells (PEMFCs) have been considered as promising alternative power sources for many mobile and stationary applications. Compared to the fast hydrogen oxidation at the anode, the sluggish oxygen reduction reaction (ORR) at the cathode requires high-performance catalysts. Currently, platium (Pt) nanoparticles supported on high surface area carbons remain the best catalysts for ORR. However, both instability and high cost of Pt-based catalysts represent two main obstacles limiting the commercial applications of PEMFCs. The instability of supported Pt catalysts is mainly due to the corrosion of carbon support under operation conditions and the agglomation and detachment of Pt particles, leading to a decrease in catalytic surface areas.[1] Development of corrosion-resistant supports and enhancement of the interactions between Pt and supports are two strategies to improve the cathode long-term activity.[2,3]

Besides the challenges to improve catalyst stabilities, it is highly desirable to search innovative cost-effective cathode catalytic materials with a high activity because of the high cost and limited availability of Pt.[4] There has been a significant activity in reducing Pt loading and replacing Pt by other catalysts.[5−7] Of many different catalysts developed so far, heat-treated nitrogen-coordinated iron on a carbon matrix (Fe/N/C) has been recognized as a promising Pt-free catalyst with potential to match the performance of Pt-based catalysts, although the stability of these novel nonprecious metal catalysts under acidic conditions requires to be improved.[8] However, some nitrogen-containing carbon nanostructures also retain a significant ORR activity even after removal of metal components.[9,10] These results suggest that metal species (e.g., iron) may not act as an active site but rather play a role to facilitate the formation of stable nitrogen sites. Moreover, nitrogen- and/or boron-doped carbons without any metal component (referred to as carbon alloy catalysts) also show ORR activities, indicating an active site does not involve any metal species.[11,12] The pyridinic type nitrogen is generally considered to be responsible for the active sites,[9] but recent study suggests that graphitic type nitrogen species are the key to inducing catalytic activities.[13] Therefore, a fundamental understanding of the roles of nitrogen doping is of great benefit toward a rational design of Pt-free cathode catalytic materials. Compared to the catalysts prepared with metal, the carbon alloy catalyst system would serve as a simpler model without taking account of the effects of any metal species.

Doping nitrogen on carbon materials is usually fulfilled via treatment of carbons by gaseous NH_3 or HCN. Previous study has shown that the nature of the pristine carbons has a great effect on the ORR activities of the treated carbons.[14] We and others have recently developed

*Corresponding author. E-mail: dais@ornl.gov.

(1) (a) Borup, R.; Meyers, J.; Pivovar, B.; et al. *Chem. Rev.* **2007**, *107*, 3904. (b) Shao-Horn, Y.; Sheng, W. C.; Chen, S.; Ferreira, P. J.; Holby, E. F.; Morgan, D. *Top. Catal.* **2007**, *46*, 285.
(2) (a) Wang, X.; Li, W. Z.; Chen, Z. W.; Waje, M.; Yan, Y. S. *J. Power Sources* **2006**, *158*, 154. (b) Shanahan, P. V.; Xu, L. B.; Liang, C. D.; Waje, M.; Dai, S.; Yan, Y. S. *J. Power Sources* **2008**, *185*, 423. (c) Shao, Y. Y.; Zhang, S.; Kou, R.; Wang, X. Q.; Wang, C. M.; Dai, S.; Viswanathan, V. V.; Liu, J.; Wang, Y.; Lin, Y. H. *J. Power Sources.* **2010**, *195*, 1805.
(3) (a) Zhu, Q.; Zhou, S. H.; Wang, X. Q.; Dai, S. *J. Power Sources* **2009**, *193*, 495. (b) Zhong, H.; Xiang; Zhang, H. M.; Liang, Y. M.; Zhang, J. L.; Wang, M. R.; Wang, X. L. *J. Power Sources* **2007**, *164*, 572. (c) Donthu, S.; Cai, M.; Ruthkosky, M.; Halalay, I. *Chem. Commun.* **2009**, 4203.
(4) (a) Bezerra, C. W. B.; Zhang, L.; Lee, K. C.; Liu, H. S.; Marques, A. L. B.; Marques, E. P.; Wang, H. J.; Zhang, J. J. *Electrochim. Acta* **2008**, *53*, 4937. (b) Shao, Y. Y.; Sui, J. H.; Yin, G. P.; Gao, Y. Z. *Appl. Catal., B* **2008**, *79*, 89.
(5) (a) Zhang, J. L.; Vukmirovic, M. B.; Sasaki, K.; Nilekar, A. U.; Mavrikakis, M.; Adzic, R. R. *J. Am. Chem. Soc.* **2005**, *127*, 12480. (b) Stamenkovic, V. R.; Fowler, B.; Mun, B. S.; Wang, G. F.; Ross, P. N.; Lucas, C. A.; Markovic, N. M. *Science* **2007**, *315*, 493. (c) Koh, S.; Strasser, P. *J. Am. Chem. Soc.* **2007**, *129*, 12624.
(6) (a) Lee, K.; Zhang, L.; Zhang, J. J. *Electrochem. Commun.* **2007**, *9*, 1704. (b) Lewera, A.; Inukai, J.; Zhou, W. P.; Cao, D.; Doung, H. T.; Alonso-Vante, N.; Wieckowski, A. *Electrochim. Acta* **2007**, *52*, 5759. (c) Ziegelbauer, J. M.; Murthi, V. S.; O'Laoire, C.; Guila, A. F.; Mukerjee, S. *Electrochim. Acta* **2008**, *53*, 5587.
(7) (a) Bashyam, R.; Zelenay, P. *Nature* **2006**, *443*, 63. (b) Yuasa, M.; Yamaguchi, A.; Itsuki, H.; Tanaka, K.; Yamamoto, M.; Oyaizu, K. *Chem. Mater.* **2005**, *17*, 4278.
(8) (a) Lefevre, M.; Proietti, E.; Jaouen, F.; Dodelet, J. P. *Science* **2009**, *324*, 71. (b) Lefevre, M.; Dodelet, J. P.; Bertrand, P. *J. Phys. Chem. B* **2000**, *104*, 11238. (c) Jaouen, F.; Lefevre, M.; Dodelet, J. P.; Cai, M. *J. Phys. Chem. B* **2006**, *110*, 5553. (d) Jaouen, F.; Marcotte, S.; Dodelet, J. P.; Lindbergh, G. *J. Phys. Chem. B* **2003**, *107*, 1376.
(9) (a) Matter, P. H.; Wang, E.; Ozkan, U. S. *J. Catal.* **2006**, *243*, 395. (b) Matter, P. H.; Ozkan, U. S. *Catal. Lett.* **2006**, *109*, 115. (c) Matter, P. H.; Wang, E.; Arias, M.; Biddinger, E. J.; Ozkan, U. S. *J. Mol. Catal., A* **2007**, *264*, 73.
(10) Gong, K. P.; Du, F.; Xia, Z. H.; Durstock, M.; Dai, L. M. *Science* **2009**, *323*, 760.
(11) (a) Ozaki, J. I.; Tanifuji, S. I.; Kimura, N.; Furuichi, A.; Oya, A. *Carbon* **2006**, *44*, 1324. (b) Ozaki, J.; Anahara, T.; Kimura, N.; Oya, A. *Carbon* **2006**, *44*, 3358. (c) Ozaki, J.; Kimura, N.; Anahara, T.; Oya, A. *Carbon* **2007**, *45*, 1847.
(12) Subramanian, N. P.; Li, X. G.; Nallathambi, V.; Kumaraguru, S. P.; Colon-Mercado, H.; Wu, G.; Lee, J. W.; Popov, B. N. *J. Power Sources* **2009**, *188*, 38.
(13) (a) Ikeda, T.; Boero, M.; Huang, S. F.; Terakura, K.; Oshima, M.; Ozaki, J. *J. Phys. Chem. C* **2008**, *112*, 14706. (b) Niwa, H.; Horiba, K.; Harada, Y.; Oshima, M.; Ikeda, T.; Terakura, K.; Ozaki, J.; Miyata, S. *J. Power Sources* **2009**, *187*, 93.
(14) (a) Jaouen, F.; Charreteur, F.; Dodelet, J. P. *J. Electrochem. Soc.* **2006**, *153*, A689. (b) Charreteur, F.; Jaouen, F.; Ruggeri, S.; Dodelet, J. P. *Electrochim. Acta* **2008**, *53*, 2925.

 Published on Web 03/19/2010

Table 1. Textural Properties and Gas Permeance of Surface-Etched Mesoporous Carbon Membranes

materials	yield (%)	S_{BET} (m_2/g)[a]	w (nm)[b]	V_t (cm^3/g)[c]	V_{micro} (cm^3/g)[c]	V_{meso} (cm^3/g)[c]	N content (%)[d]	percentage (%) pyridinic	percentage (%) graphitic	E_{onset} (mV)[e]	n[f]
C-ORNL-1		658 (362)	6.9	0.63	0.17	0.46	0				
N-OMC-950	37.4	1681 (690)	6.5	1.59	0.39	1.20	6.0 ± 0.3	44.0	8.6	669	3.48
N-OMC-1000	23.4	2121 (482)	6.6	2.15	0.47	1.68	3.6 ± 0.3	45.2	9.0	703	3.72
N-OMC-1050	4.0	1923 (229)	4.0	2.11	0.42	1.69	4.6 ± 0.4	46.9	10.0	720	3.41

[a] S_{BET}: BET surface area. The numbers in paratheses are micropore surface areas, calculated by the *t* plot method. [b] w: BJH mesopore diameter. [c] V_t, V_{micro}, V_{meso}: total pore volume, micropore volume, and mesopore volume, respectively. [d] Determined by XPS. [e] Onset potential (vs NHE) is referred as the point of 5% increase in current. The onset potential of Pt-20 is 799 mV. [f] n: electron transfer number. Under identical conditions, Pt-20 shows an electron transfer number of 3.88.

a general soft-template strategy toward synthesis of mesoporous carbon materials.[15−17] The unique structural feature of these mesoporous carbons is that the micropores embedded in the mesopore walls are more easily accessible to gaseous activation molecules than those of the conventional microporous carbons, resulting in more efficient activation processes with a homogeneous distribution of functionalized sites. In addition, ordered mesoporous carbons with a high surface area and a uniform pore size facilitate the access of reactants to the active sites and allow a good reactant flux.[18] Herein, we report the synthesis of nitrogen-doped ordered mesoporous carbons via NH_3 activation as alternative metal-free catalysts, which exhibit a significant ORR activity in acidic media. Moreover, these new catalysts exhibit a better stability than a commercial Pt/Vulcan X-72 catalyst (20 wt % Pt on Vulcan X72R from ElectroChem, Inc., denoted as Pt-20 herein).

Nitrogen-doped catalysts were prepared by heat treatment of a 2D hexagonal ordered mesoporous carbon (denoted as C-ORNL-1[16]) under flowing NH_3 at high temperatures (e.g., 950−1050 °C) for 1 h. The reactions between carbon and NH_3 involve the replacement of oxygen-bearing species by nitrogen-containing groups and the etching of carbon fragments by the radicals generated by the decomposition of NH_3 at elevated temperatures.[19] The yield was found to be dependent on the heat-treatment temperature (Table 1).

Figure 1 shows the N_2 sorption isotherms and the BJH mesopore size distribution plots of the pristine (hexagonal C-ORNL-1) and NH_3 heat-treated carbon materials (denoted as N-OMC-*x*, where *x* is the heat-treatment temperature). It is clear that after NH_3 treatment at high temperatures, both BET surface area and pore volume of N-OMC-*x* increase compared to the pristine carbon material (see also Table 1). There is little change on mesopore size for the samples N-OMC-950 and N-OMC-1000, compared to untreated C-ORNL-1, suggesting that the

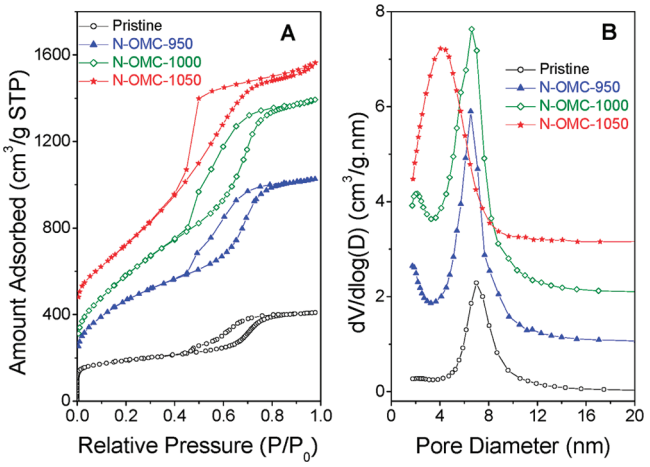

Figure 1. (A) N_2 sorption isotherms at 77 K and (B) BJH mesopore size distribution plots of the pristine and N-OMC-*x* carbons. For clarity, the isotherm N-OMC-1050 was shifted up by 200 cm^3/g STP and the PSD plots of N-OMC-950, N-OMC-1000, and N-OMC-1050 were shifted up by 1, 2, and 3 cm^3/(g nm), respectively.

ordered mesostructure is well-preserved under NH_3 treatment when the treatment temperature is not over 1000 °C. When the NH_3 treatment temperature further increases to 1050 °C, the mesopore-size distribution broadens and the average mesopore size decreases, indicating a degradation of the corresponding ordered structure while the mesoporous structure of N-OMC-1050 still remains, as revealed by TEM images (Figure S1, see the Supporting Information). Accordingly, with an increase in NH_3 treatment temperature the BET surface area and pore volume of the resulting carbon materials increase to 2068 m^2/g and 2.15 cm^3/g for N-OMC-1000, followed by a decrease to 1855 m^2/g and 2.11 cm^3/g for N-OMC-1050. Furthermore, as the treatment temperature increases, the contribution to the total surface area from micropore decreases; however, the treated carbons exhibit an increasing mesopore surface area (Table 1).

Figure 2 shows the polarization curves of oxygen reduction on N-OMC-*x*. For comparison, the curves on the pristine C-ORNL-1 and the commercial Pt catalyst (Pt-20) are also shown. The pristine C-ORNL-1 shows a very poor oxygen reduction reaction (ORR) activity, whereas N-OMC-950 exhibits significantly enhanced ORR activity. The ORR activity further increases with the increasing NH_3 treatment temperature, reaching an onset positional at about 720 mV (vs NHE) on N-OMC-1050. This reduction potential is about 80 mV below that of the commercial Pt catalyst (Pt-20), which shows the

(15) (a) Liang, C. D.; Li, Z. J.; Dai, S. *Angew. Chem., Int. Ed.* **2008**, *47*, 3696. (b) Liang, C. D.; Dai, S. *J. Am. Chem. Soc.* **2006**, *128*, 5316.
(16) Wang, X. Q.; Liang, C. D.; Dai, S. *Langmuir* **2008**, *24*, 7500.
(17) (a) Tanaka, S.; Nishiyama, N.; Egashira, Y.; Ueyama, K. *Chem. Commun.* **2005**, 2125. (b) Meng, Y.; Gu, D.; Zhang, F. Q.; Shi, Y. F.; Yang, H. F.; Li, Z.; Yu, C. Z.; Tu, B.; Zhao, D. Y. *Angew. Chem., Int. Ed.* **2005**, *44*, 7053–7059.
(18) (a) Chang, H.; Joo, S. H.; Pak, C. *J. Mater. Chem.* **2007**, *17*, 3078. (b) Antolini, E. *Appl. Catal., B* **2009**, *88*, 1.
(19) (a) Stohr, B.; Boehm, H. P.; Schlogl, R. *Carbon* **1991**, *29*, 707. (b) Mangun, C. L.; Benak, K. R.; Economy, J.; Foster, K. L. *Carbon* **2001**, *39*, 1809.

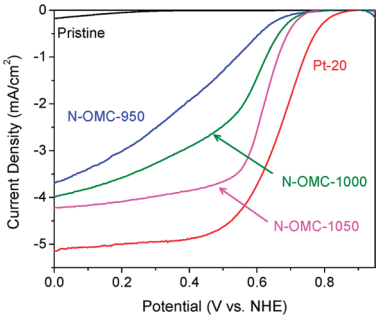

Figure 2. Polarization curves of oxygen reduction on N-OMC-*x*. For comparison, the curves on the pristine OMC and a commercial platinum catalyst (20 wt % Pt) are also included. ORR tests were carried out in oxygen-saturated 0.05 M H_2SO_4, the rotation rate of RDE was 1600 rpm, and the potential scan rate was 10 mV/s. Nonfaradaic currents obtained in N_2 saturated electrolyte under identical conditions were subtracted. Catalysts loading for Pt-20 and N-OMC-*x* were 352 and 312 μg/cm^2, respectively.

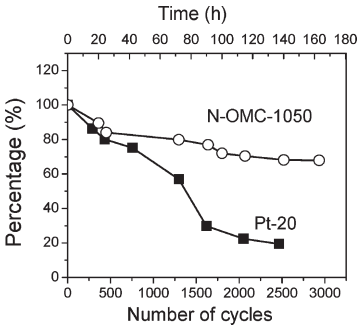

Figure 3. Comparison of stability of N-OMC-1050 and Pt-20 in terms of the retention percentage of the current at 0.72 and 0.80 V, respectively.

onset potential at 799 mV (vs NHE), but still higher than other metal-free N-doped carbon based catalysts reported previously.[11,12] Using the Koutechy−Levich equation, the electron transfer numbers were calculated (see Figure S2 in the Supporting Information). For both Pt-20 and N-OMC-*x*, the electron transfer numbers calculated based on the respectively measured diffusion limiting current (I_{dl}) are close to 4 (Table 1), suggesting that the O_2 reduction catalyzed by these electrocatalysts mainly follows the 4e reduction mechanism.

To exclude the possibility of ORR activities induced by trace amount of metal species, we characterized our catalysts via both X-ray photoelectron spectroscopy (XPS) and inductively coupled plasma (ICP) spectrometer. XPS spectra show no detectable metal species and ICP analyses suggest that the Fe content, if present, is below 100 ppm. Previous studies have shown that an effective Fe/N/C electrocatalyst contained more than 0.2 wt % Fe (2000 ppm).[8,14] Therefore, the ORR activity of ammonia-treated OMCs is ascribed to the presence of active nitrogen species. To investigate the chemical states of the doped nitrogen atoms, we performed narrow scan N1s XPS analyses. No nitrogen signal was observed for the pristine carbon, while about 4−6 at % of nitrogen was detected for N-OMC-*x* (Figure S3). The N 1s signals can be deconvoluted into 5 different types of nitrogen species, i.e., pyridinic-type (~398.5 eV), nitrile or imine (~ 399.5 eV), pyrrolic-type (~400.5 eV), graphitic-type (~401.3 eV) nitrogen, and oxidized nitrogen (402−405 eV) (also see Table 1).[9,19] It is clear that all of three NH_3 treated samples contain large percentages of both pyridinic and graphitic types of nitrogen, which are believed to be responsible for the active sites. Interestingly, N-OMC-950 with the highest N content shows the lowest ORR activity among the three NH_3-treated samples. This observation is likely due to the presence of considerable micropore surface area of N-OMC-950 (Table 1), which is kinetically inaccessible to O_2. The increase in ORR activity of the nitrogen-modified catalysts follows the trend of their mesopore surface area. These results agree well with the previous findings[8] that both nitrogen contents and textural properties of the NH_3-treated samples have great effects on their ORR activity.

To investigate the electrochemical stability of N-OMC-1050, we performed extended voltage cycling within a potential range of 0 to 1.0 V (vs NHE) in 0.05 M H_2SO_4 at room temperature. During different cycle intervals, linear sweep voltammetry was carried out in oxygen-saturated 0.05 M H_2SO_4. The stability is described in terms of the retention percentage of the ORR current at their onset potential points. As shown in Figure 3, after ~2000 cycles (120 h), N-OMC-1050 still retained more than 70% of its initial current density. This observation is in sharp contrast to the performance of Pt-20 under idential conditions, which showed a quick loss in current with about 20% remained after 120 h. This result clearly indicates that N-OMC-1050 is much more stable than the Pt-based electrocatalysts. The higher stability of N-OMC-1050 is attributed to the nature of its active sites, which are induced by nitrogen doping and are less amenable to change by carbon corrosion and other degradation mechanisms that Pt supported catalysts suffer.[1] We also tested the possible crossover and poison effects of carbon monoxide (CO) on the activity of N-OMC-1050 and found that it exhibited a much higher resistance to CO poisoning than Pt-20 because of the the characteristic of nonmetal active sites[10] for the former (see Figure S4 in the Supporting Information).

In summary, we have prepared alternative nonmetal ORR catalysts via NH_3 heat treatment of ordered mesoporous carbons that exhibit high activity and good stability. We expect that this finding would have a considerable impact on the development of advanced Pt-free catalytic materials to meet the requirements of ORR catalysts toward wide applications of PEMFCs.

Acknowledgment. This research was sponsored by the Office of Energy Efficiency and Renewable Energy (EERE), U.S. Department of Energy, under Contract DE-AC05-0096OR22725 with Oak Ridge National Laboratory, managed and operated by UT-Battelle, LLC.

Supporting Information Available: Experimental and characterization details, and Figures S1−S4 (PDF). This material is available free of charge via the Internet at http://pubs.acs.org.